A CONTINUUM DESCRIPTION OF VASCULAR TUMOR GROWTH

Anna Claudia M. Resende

Regina C. Almeida

Brendon J. Rodrigues

annacmr@lncc.br

rcca@lncc.br

bjesus@lncc.br

Laboratório Nacional de Computação Científica (LNCC/MCTI)

Av. Getúlio Vargas 333, 25651-075, Petrópolis, Rio de Janeiro, Brazil

Ernesto A. B. F. Lima

lima@ices.utexas.edu

Institute for Computational Engineering and Sciences (ICES)

201 East 24th St., 78712-1229, Austin, Texas, USA

Abstract. *Angiogenesis, the creation of new blood vessels, is a key mechanism of carcinogenesis. During the early stages of a tumor progression, called avascular phase, highly proliferative cancer cells quickly exhausts nutrient availability in the microenvironment, eventually leading to growth arrest. Nutrient stress gives rise to hypoxic cells that, to overcome nutrient depletion, secrete tumor angiogenic factors, which ultimately induce the growth of new blood vessels. The new vascular network not only resumes tumor growth but also provides unbound conditions to sustain tumor progression, switching tumors to the more aggressive vascular phase. In this work we model this phenomenon using mass conservation principles. We build a vascular model in a highly heterogeneous microenvironment, including tumor and healthy cells competition and their interplay with extracellular matrix. A sensitivity analysis performed in the model indicates that the competition for space and resources, and the creation of new blood vessels have significant impact on the tumor evolution.*

Keywords: *Mathematical Model, Tumor Growth, Angiogenesis.*

1 INTRODUCTION

Cancer progression and invasion are complex processes involving interaction between different cell types. In order to grow, tumor cells remodel their microenvironment by interacting with the extracellular matrix and promoting the growth of new blood vessels for diffusion exchange of nutrients. This is required not only due to the increased nutrient consumption by tumor cells but also the competition between healthy and tumor cells. This interaction has been studied in the literature focusing on population dynamic models (Brown & Rothery, 1993; Kirschner & Panetta, 1998; Nani & Freedman, 2000; Sachs *et al.*, 2001), and including spatial heterogeneity (André *et al.*, 2013; Hubbard & Byrne, 2013; Oden *et al.*, 2016). Recent studies have shown that competition between healthy and cancerous cells is crucial on cancer remission and cancer relapse (MacLean *et al.*, 2014). Therefore, the objective of this work is to develop a mathematical model to describe the growth of solid tumors, including the mechanisms related to the transition between avascular and vascular phases. Using mass conservation principles, our model encompasses the dynamics of tumor, healthy and endothelial cells, degradation and regeneration of the extracellular matrix (ECM), and diffusion of oxygen, vascular endothelial growth factor (VEGF), and matrix degrading enzymes. Tumor cells are split into proliferative, hypoxic and dead cells. Hypoxic cells trigger angiogenesis by secreting angiogenic factors, represented here by the VEGF concentration. This factor stimulates the growth of endothelial cells, providing a positive feedback for the oxygen supply. Since we are using the continuum framework, we do not track the growth of new vessels. Instead, they are expressed by the continuum concentration of endothelial cells. All cells are embedded in the ECM, which provides structural substrate for cell adhesion and tissue development (Bonnans *et al.*, 2014). In order to migrate, cancer cells release matrix degrading enzymes, such as matrix metalloproteinases, that degrade the ECM, providing free space for cancer growth. At the same time, proliferative cells act on ECM remodeling to guarantee structural integrity. Overall, the mathematical model is represented by a coupled system of nine nonlinear partial differential equations. This model extends previous works (Hinow *et al.*, 2009; Resende, 2016; Souza, 2013), aiming at representing the intricate process of vascular tumor growth. In section 2 we describe the model in details and provide the main procedures for getting its numerical solution. The following section presents some preliminary simulations in order to illustrate the general behavior of the model in one-dimensional spatial domains. Specifically, we focus on the tumor and healthy cells interactions, the ECM dynamics and how the angiogenesis impact the tumor progression. We also perform a model-free sensitivity analysis to study the impact of parameter uncertainties on the tumor evolution. We focus on the identification of the set of influential parameters with respect to the tumor volume evolution, recognized as a meaningful quantity of interest (QoI). The uncertainty analysis is performed through the screening Elementary Effects (EEs) Method (Morris, 1991; Saltelli *et al.*, 2008). Section 4 concludes the paper.

2 MATHEMATICAL MODEL

The general basis for constructing the model is the one built in Hinow *et al.* (2009). Among other features, our model explicitly includes tumor and healthy cells competition, which seems to play crucial role in tumor progression. We assume that the tumor microenvironment is fully occupied by tumor cells, healthy or normal cells, endothelial cells and ECM, so that

$$v = T + F + E + N, \tag{1}$$

in which T, E, N and F stand for the density of tumor, endothelial, and normal cells, and ECM. The total tumor cell density (T) is composed by proliferative (P), hypoxic (H) and dead (D) cells. We assume that proliferative cells encompass both quiescent and cells undergoing mitosis, while dead cells results only from oxygen depletion. Considering that oxygen diffuses through the microenvironment from original blood vessels, those different tumor phenotypes are defined by oxygen availability. We denote the oxygen concentration by O and define O_h and O_d as the thresholds bellow which tumor cells become hypoxic or dead, respectively. Matrix degrading enzymes (M) are assumed to be soluble, so that they diffuse in the microenvironment, as well as the vascular endothelial growth factor (G).

By considering a typical size of an early stage tumor, a typical cell cycle duration, maximum cell density, background oxygen concentration and VEGF saturation, our nondimensional model defined in $\Omega \times (0, \tau_{max}]$ is given by the following set of equations:

$$
\mathcal{M}: \begin{cases}
\dfrac{\partial O}{\partial t} = \boldsymbol{\nabla} \cdot (\boldsymbol{D}_o \boldsymbol{\nabla} O) + \alpha_o E(1-O) - \beta_o^p (P+H)O - \beta_o^n (E+N)O; \\
\dfrac{\partial N}{\partial t} = \boldsymbol{\nabla} \cdot (\boldsymbol{D}_n \boldsymbol{\nabla} N) + \alpha_n NFO \max\{1-v, 0\} - \gamma_n NP; \\
\dfrac{\partial P}{\partial t} = \boldsymbol{\nabla} \cdot (\boldsymbol{D}_p \boldsymbol{\nabla} P) + \alpha_p PFO \max\{1-v, 0\} - \alpha_h \mathcal{H}(O_h - O)P + h_p \alpha_h \mathcal{H}(O-O_h)H; \\
\dfrac{\partial H}{\partial t} = \boldsymbol{\nabla} \cdot (\boldsymbol{D}_h \boldsymbol{\nabla} H) - h_p \alpha_h \mathcal{H}(O-O_h)H + \alpha_h \mathcal{H}(O_h - O)P - \beta_h \mathcal{H}(O_d - O)H; \\
\dfrac{\partial D}{\partial t} = \boldsymbol{\nabla} \cdot (\boldsymbol{D}_d \boldsymbol{\nabla} D) + \beta_h \mathcal{H}(O_d - O)H; \\
\dfrac{dF}{dt} = -\beta_f MF + \alpha_f P \max\{1-v, 0\}; \\
\dfrac{\partial M}{\partial t} = \boldsymbol{\nabla} \cdot (\boldsymbol{D}_m \boldsymbol{\nabla} M) + \alpha_m P \max\{1-M, 0\} - \beta_m M - \beta_f MF; \\
\dfrac{\partial E}{\partial t} = \boldsymbol{\nabla} \cdot (\boldsymbol{D}_e \boldsymbol{\nabla} E) + \alpha_e EG \max\{1-v, 0\}; \\
\dfrac{\partial G}{\partial t} = \boldsymbol{\nabla} \cdot (\boldsymbol{D}_g \boldsymbol{\nabla} G) + \alpha_g H \max\{1-G, 0\} - \beta_g EG; \\
v = P + H + D + F + E + N.
\end{cases}
$$

Excluding the ECM, all constituents, chemicals and growth factors have random spatial motility proportional to constant isotropic diffusions, for simplicity. Oxygen supply comes from the blood vessels at a rate α_o up to the maximum background concentration. Unlike in Hinow *et al.* (2009), we assume that the uptake rate of oxygen by viable tumor cells β_o^p is much higher than that by endothelial and healthy cells β_o^n. In order to proliferate, both healthy and tumor cells depend on the availability of substrate (F), oxygen, and space, defined by the term $\max\{1-v,\ 0\}$. Healthy cells undergo competitive inhibition due to the presence of proliferative cells, whose strength is given by γ_n. Tumor phenotype transitions are provided by the Heaviside function $\mathcal{H}$, which is one for positive arguments and zero otherwise. Matrix

degrading enzymes (M) are produced by proliferative cells at a rate α_m, up to a saturation concentration, and undergo a natural decay at a rate β_m. ECM degradation leads to a decrease of M at a rate β_f (Deakin & Chaplain, 2013). Another new feature of our modeling is the ECM remodeling by proliferative cells at a rate α_f, subject to space availability. Tumor-associated angiogenesis is trigged by the VEGF secreted by hypoxic cells at a rate α_g, up to the maximum background concentration. Eventually, VEGF concentration regulates the growth of endothelial cells at a rate α_e, and in accordance with space availability. This yields a decrease in VEGF concentration at a rate β_g. Table 1 shows the values and meanings of each parameter of $\mathcal{M}$. Most of them are estimated, while others are extracted from Hinow *et al.* (2009).

Table 1: Nondimensional parameter vector ($\bar{X}$) for model $\mathcal{M}$. Bold values are estimated for this work, while the others are extracted from Hinow *et al.* (2009).

$\bar{X}$	Value	Meaning	$\bar{X}$	Value	Meaning
D_o	0.58	nutrient diffusion coeff.	α_f	**0.3**	rate of ECM growth
D_n	$\mathbf{5.8 \times 10^{-5}}$	normal cells diffusion coeff.	α_e	**0.7**	rate of endothelial cells growth
D_p	5.8×10^{-5}	proliferative cells diffusion coeff.	α_g	10.0	rate of VEGF growth
D_h	$\mathbf{1.0 \times 10^{-5}}$	hypoxic cells diffusion coeff.	β_o^p	0.57	oxygen consumption rate
D_d	$\mathbf{1.0 \times 10^{-6}}$	dead cells diffusion coeff.	β_o^n	**0.04**	oxygen consumption rate
D_m	**0.1**	MDE diffusion coeff.	β_h	0.32	transfer rate from h to d
D_e	5.8×10^{-5}	endothelial cells diffusion coeff.	β_f	0.5	rate of ECM degradation
D_g	0.02	VEGF diffusion coeff.	β_m	**10.0**	MDE decay rate
α_o	1.0	rate of oxygen growth	β_g	**5.0**	VEGF consumption rate
α_n	$\mathbf{1.0 \times 10^{-3}}$	rate of normal cells prolif.	O_h	**0.4**	threshold p to h
α_p	**3.0**	rate of proliferative cells growth	O_d	**0.3**	threshold h to d
α_h	1.6	transfer rate from p to h	h_p	0.1	% transfer rate from h to p
α_m	**7.0**	rate of MDE growth	γ_n	**0.5**	competition between normal and prolif. cells

3 NUMERICAL SIMULATION

In this section, we conduct a numerical experiment in order to verify the main features and behavior of the model presented in Section 2. The approximate solution to system $\mathcal{M}$ is solved by using the finite element method (FEM) and the implicit Euler method to approximate the time derivatives. Due to the dominance of reactive effects in the hypoxic and dead cells equation, a stabilized FEM is required. The system is linearized by using Picard's method and is solved uncoupling the equations through a Gauss-Seidel strategy (see Resende (2016) for details). The resulting discrete forms are implemented in C++ using the open source `libMesh` library (Kirk *et al.*, 2006).

For this experiment, we consider a small tumor mass growing inside a 1D normal tissue. Due to symmetry, we solve only half of the spatial domain given by $\Omega = (-3, 3)$. Thus, the region $\Omega = (0, 3)$ is partitioned into 400 uniform elements. The time domain $(0, \tau_{max}]$ is also split into uniform time steps $\Delta t = 0.1$, and we set $\tau_{max} = 600$. We remark that these discretization parameters are small enough to guarantee convergent solutions. No flux (Neumann) boundary conditions are stated except for a fixed oxygen supply at the right corner of the domain ($x = 3.0$). At $t = 0$, we assume that oxygen exists at its maximum concentration throughout

the domain, and there are no hypoxic cells, and VEGF and matrix degrading enzymes concentrations. Basal values are stated for dead, endothelial cells and ECM. Normal cells density is obtained by satisfying (1). Specifically, initial conditions are the following:

$$\mathcal{IC}: \begin{cases} O(x,0) = 1.0; \\ N(x,0) = 1.0 - P(x,0) - H(x,0) - D(x,0) - F(x,0) - E(x,0); \\ P(x,0) = 0.93e^{-200x^2}; \\ H(x,0) = 0.0; \\ D(x,0) = 5.0 \times 10^{-2}; \\ F(x,0) = 2.0 \times 10^{-1}; \\ M(x,0) = 0.0; \\ E(x,0) = 1.0 \times 10^{-2}; \\ G(x,0) = 0.0. \end{cases}$$

The tumor evolution is shown in Fig. 1 for four different times. Figure 1(a) depicts the initial condition for all model's constituents. Figure 1(b) shows the avascular phase of the tumor growth. Matrix degrading enzymes are released by cancer cells to degrade ECM and provide space for growth. We also notice a slight regeneration at the tumor front caused by the action of proliferative cells on ECM to ensure cell adhesion and tissue development. Normal cells exist in regions where there is no tumor due to the strong competitive inhibition by proliferative cells. Figure 1(c) shows that the intense growth leads to an insufficient oxygen supply to maintain the proliferation process, causing the emergence of hypoxic cells. These cells secrete VEGF and induce the growth of endothelial cells, characterizing the vascular phase of tumor growth, but angiogenesis is not sufficient to increase the nutrient availability to sustain this intense growth. Eventually, dead cells appear, so that at $t = 600$ a cluster of dead cells is concentrated in the middle of the domain, as depicted in Fig. 1(d). We also remark the increase of proliferative cells from $t = 400$ to $t = 600$, accompanied by the growth of MDEs and the spread of new blood vessels. As highlighted in Fig. 2, the VEGF concentration appears together with the onset of hypoxic cells.

The parameters used in the simulation are quite uncertain. To investigate how their uncertainties impact the tumor evolution, we perform a sensitivity analysis using the model-free screening Elementary Effects method (Morris, 1991; Saltelli *et al.*, 2008). We assume that each parameter follows a continuous uniform distribution $\mathcal{U}(0.8\bar{X}_i, 1.2\bar{X}_i)$, in which $\bar{X}_i$ stands for its corresponding mean value shown in Table 1. Although there are 26 parameters in this table, only $d = 25$ are independent since O_h must be larger than O_d. In particular, we sample O_h and then set $O_d = O_h - 0.1$ in order to guarantee that $O_h > O_d$. The elementary effects method provides two sensitivity measures for each parameter considered in the analysis: the average μ_i^* and the standard deviation σ_i. The former indicates the overall importance of the selected parameter while the latter depicts its nonlinear interaction role regarding other parameters of the model, with respect to the selected quantity of interest. Here the tumor volume is chosen as a meaningful QoI. The EEs indexes are obtained here by performing a screening of the parametric space through $r = 20$ trajectories of $(d + 1)$ points according to specific rules, beginning with a base vector randomly sampled in a p-level grid ($p = 4$) (see Resende (2016) and Saltelli *et al.* (2008) for more details). Figure 3 shows the sensitivity analysis indexes for all parameters considered

in the analysis. We notice that almost all parameters of the model are considered important. The analysis points out that the dynamics of proliferative and normal cells, oxygen, and ECM play prominent roles in the tumor volume evolution. It can be seen, for example, that the diffusion coefficient and the growth rate of proliferative cells (D_p, α_p), the competition rate between normal and proliferative cells (γ_n), and the oxygen uptake rate of tumor cells (β_o^p) are the most influential parameters with respect to the selected QoI, also displaying strong nonlinear roles. On the other hand, D_h and D_d are identified as not important because their both μ^* and σ values are very small. Biologically, these hypoxic and dead cells diffusion coefficients are associated with the mobility gain due to hypoxic conditions and exudative inflammation caused by tissue necrosis, respectively (Souza, 2013). Here D_h and D_d are set much smaller than D_p and play

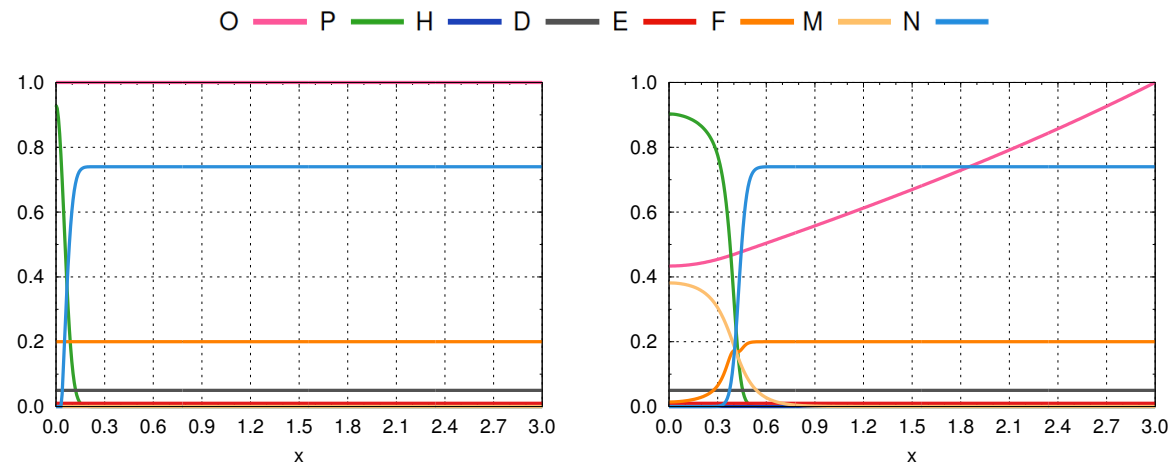

(a) Simulation time: t = 0. Initial condition of the model represents a small tumor mass growing inside a 1D normal tissue.

(b) Simulation time: t = 100. Matrix degrading enzymes are released by cancer cells to degrade ECM and provide space for the tumor growth.

(c) Simulation time: t = 400. The intense growth leads to an insufficient oxygen supply towards the center of the tumor, causing the onset of hypoxic cells, the establishment of the angiogenesis, and the increase of endothelial cells.

(d) Simulation time: t = 600. Angiogenesis sustains rapid tumor growth, although it is not sufficient to keep oxygen availability at the tumor center. Eventually, a central core of dead cells appear.

Figure 1: Simulation of the tumor evolution for four different times, that highlight the two main stages of the tumor growth: the avascular (a, b) and vascular (c, d) phases of cancer. Spatial position is displayed on the x-axis, and the y-axis displays the concentrations of the model constituents according with the color bar indicated at the top of this figure.

important roles on the numerical scheme stability around the onset of hypoxic and dead cells. Likewise, the parameters D_m, α_m and β_m that appear in the MDE equation are also labeled not important. This may mean that the desired effect of the action of these enzymes on ECM's degradation can be modeled without modeling the MDE dynamics explicitly. Specifically, since MDE are produced by proliferative cells, we can alternatively exchange the term $-\beta_f MF$ in ECM's equation for $-\beta_f PF$, directly considering the influence of proliferative cells on ECM's degradation.

Figure 4 shows the mean and standard deviation of the tumor volume (QoI) considering the $r(d+1)$ experiments carried out in the sensitivity analysis. Notice that parameter uncertainty can strongly impact the tumor volume progression. As a comparison, two other experiments are performed considering the modification of only one parameter, α_p, while keeping all the others at their mean values. Blue and red dots in Fig. 4 indicate the tumor volume obtained by setting $\alpha_p = 3.6$ and $\alpha_p = 2.4$, that correspond to largest and smallest possible values of α_p. It is remarkable how this parameter is essential in the dynamics, producing great impact on the variation of the selected QoI. Moreover, its overall influence on the QoI does not occur in a linear way, emphasizing its nonlinear importance, which is in agreement with its corresponding high σ value.

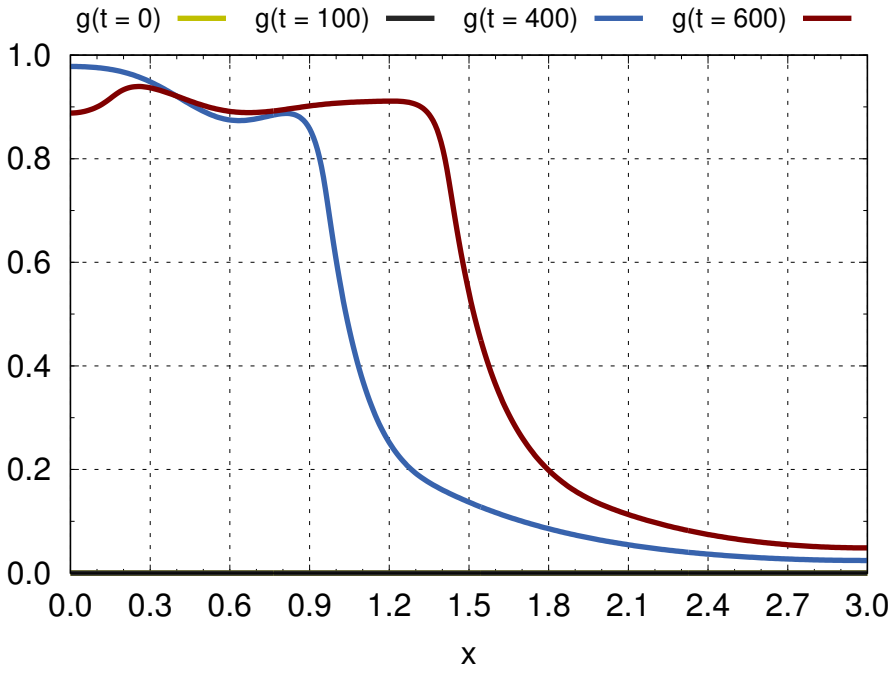

Figure 2: Spatial position is displayed on the x-axis, and the y-axis displays the concentration of VEGF at specific times of the tumor growth. Notice that the VEGF concentration appears together with the onset of hypoxic cells in the system.

4 CONCLUSION

In this work we focus on the development of a deterministic tumor growth model. Our model includes tumor and healthy cells competition, and ECM remodeling, which are considered essential features for tumor progression. Healthy cells undergo competitive inhibition due to the presence of tumor cells, while ECM is degraded to provide space for cancer growth and

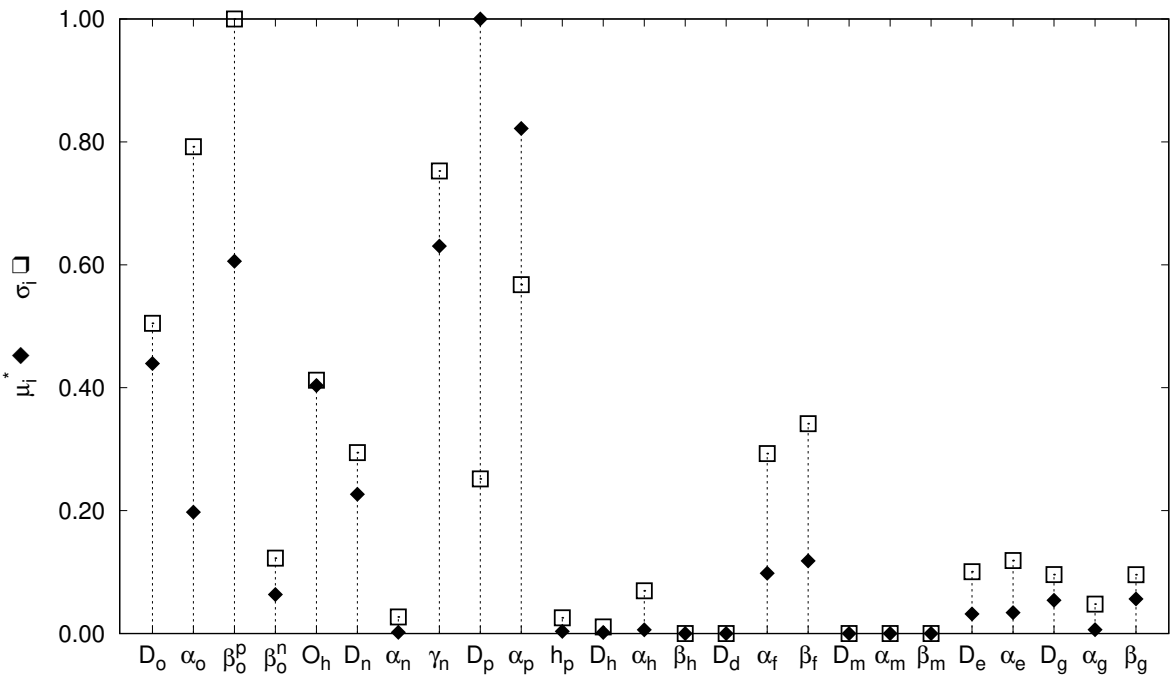

Figure 3: EEs indexes for model $\mathcal{M}$ using p = 4 subdivisions and r = 20 trajectories. The analysis points out that the dynamics of proliferative and normal cells, oxygen, and ECM play prominent roles in tumor volume evolution.

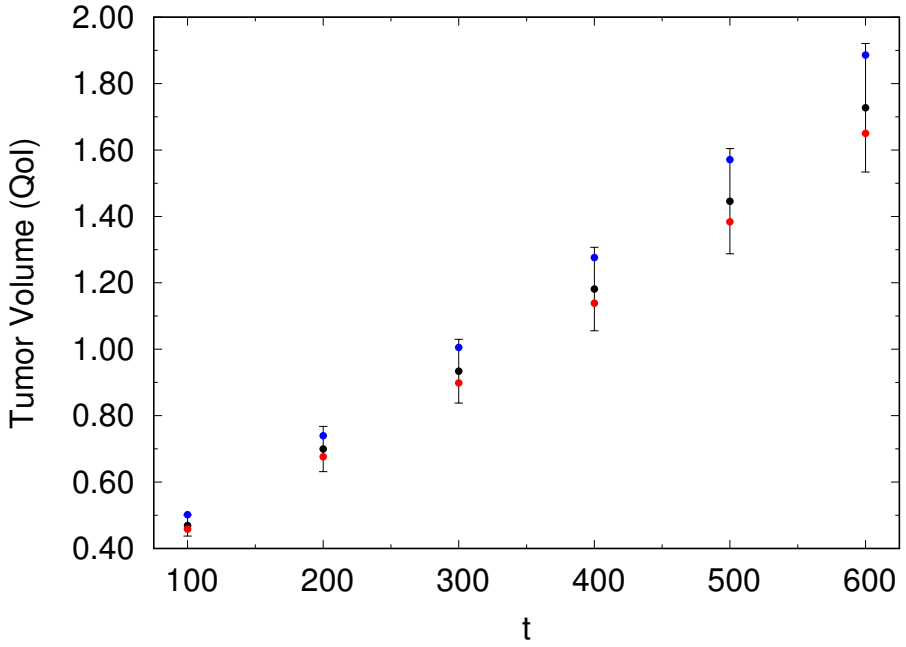

Figure 4: Mean and standard deviation of the tumor volume (QoI) considering the simulations involved in the sensitivity analysis. Guided by the analysis, we also depict the model behavior when changing only the α_p value, while keeping all other parameters at their mean values. Blue and red dots are obtained setting $\alpha_p = 3.6$ (20% greater than the mean value) and $\alpha_p = 2.4$ (20% lower), respectively. Notice the significant role of the model nonlinearities.

remodeled to guarantee structural integrity. A preliminary experiment shows both avascular and vascular tumor growth scenarios and depicts the expected general behavior of these tumor stages. We also perform a model-free sensitivity analysis to study the impact of parameter uncertainties on the tumor evolution. The analysis points out that the dynamics of proliferative and normal cells, oxygen, and ECM play prominent roles in the tumor volume modeling.

ACKNOWLEDGEMENTS

ACMR and BJR would like to thank the support through the following projects of CNPq: 132591/2014-6 and 131492/2017-9.

REFERENCES

André, N., Barbolosi, D., Billy, F., Chapuisat, G., Hubert, F., Grenier, E., & Rovini, A. 2013. Mathematical model of cancer growth controled by metronomic chemotherapies. *ESAIM: Proceedings*, **41**, 77–94.

Bonnans, C., Chou, J., & Werb, Z. 2014. Remodelling the extracellular matrix in development and disease. *Nature Reviews Molecular Cell Biology*, **15**(12), 786–801.

Brown, D., & Rothery, P. 1993. *Models in Biology: Mathematics, Statistics and Computing*. John Wiley & Sons.

Deakin, N., & Chaplain, M. A. J. 2013. Mathematical modelling of cancer invasion: the role of membrane-bound matrix metalloproteinases. *Frontiers in Oncology*, **3**(70).

Hinow, P., Gerlee, P., McCawley, L. J., Quaranta, V., Ciobanu, M., Wang, S., Graham, J. M., Ayati, B. P., Claridge, J., Swanson, K. R., Loveless, M., & Anderson, A. R. A. 2009. A spatial model of tumor-host interaction: application of chemotherapy. *Mathematical Biosciences and Engineering*, **6**(3), 521–546.

Hubbard, M. E., & Byrne, H. M. 2013. Multiphase modelling of vascular tumour growth in two spatial dimensions. *Journal of Theoretical Biology*, **316**, 70–89.

Kirk, B. S., Peterson, J. W., Stogner, R. H., & Carey, G. F. 2006. `libMesh`: a C++ Library for Parallel Adaptive Mesh Refinement/Coarsening Simulations. *Engineering with Computers*, **22**(3–4), 237–254.

Kirschner, D., & Panetta, J. C. 1998. Modeling immunotherapy of the tumorimmune interaction. *Journal of Mathematical Biology*, **37**(3), 235–252.

MacLean, A. L., Filippi, S., & Stumpf, M. P. H. 2014. The ecology in the hematopoietic stem cell niche determines the clinical outcome in chronic myeloid leukemia. *Proceedings of the National Academy of Sciences of the United States of America – PNAS*, **111**(10), 3883–3888.

Morris, M. D. 1991. Factorial Sampling Plans for Preliminary Computational Experiments. *Technometrics*, **33**(2), 161–174.

Nani, F., & Freedman, H. I. 2000. A mathematical model of cancer treatment by immunotherapy. *Mathematical Biosciences*, **163**(2), 159–199.

Oden, J. T., Lima, E. A. B. F., Almeida, R. C., Feng, Y., Rylander, M. N., Fuentes, D., Faghihi, D., Rahman, M. M., DeWitt, M., Gadde, M., & Zhou, J. C. 2016. Toward Predictive Multiscale Modeling of Vascular Tumor Growth. *Archives of Computational Methods in Engineering*, **23**(4), 735–779.

Resende, A. C. M. 2016. *Sensitivity Analysis as a Tool for Tumor Growth Modeling*. M.Phil. thesis, Laboratório Nacional de Computação Científica (LNCC/MCTI), Petrópolis/RJ, Brazil.

Sachs, R. K., Hlatky, L. R., & Hahnfeldt, P. 2001. Simple ode models of tumor growth and anti-angiogenic or radiation treatment. *Mathematical and Computer Modelling*, **33**(12), 1297–1305.

Saltelli, A., Ratto, M., Andres, T., Campolongo, F., Cariboni, J., Gatelli, D., Saisana, M., & Tarantola, S. 2008. *Global Sensitivity Analysis: The Primer*. John Wiley & Sons.

Souza, R. V. M. 2013. *Modelos de crescimento tumoral espacialmente heterogêneos com aplicação de quimioterapia*. M.Phil. thesis, Laboratório Nacional de Computação Científica (LNCC/MCTI), Petrópolis/RJ, Brazil.